ENGINEERING RESEARCH INSTITUTE
THE UNIVERSITY OF MICHIGAN
ANN ARBOR

ANALYSIS OF NONLINEAR O-TYPE BACKWARD-WAVE OSCILLATORS

TECHNICAL REPORT NO. 25

Electron Tube Laboratory
Department of Electrical Engineering

By

Joseph E. Rowe

Project 2750

CONTRACT NO. AF30(602)-1845
DEPARTMENT OF THE AIR FORCE
PROJECT NO. 4506, TASK NO. 45152
PLACED BY: THE ROME AIR DEVELOPMENT CENTER
GRIFFISS AIR FORCE BASE, NEW YORK

June, 1958

TABLE OF CONTENTS

ABSTRACT

The linear, large-C O-type backward-wave oscillator equations are formulated in this report and their solutions discussed. The nonlinear traveling-wave tube equations have been modified to permit the analysis of O-type backward-wave oscillator operation in the large-C region. These equations have been solved for large values of C including the effect of space charge.

The start-oscillation conditions are determined by assuming values of circuit voltage at the gun end and electron velocity and integrating the nonlinear equations until the circuit voltage is zero. The start-oscillation condition may occur at the first or subsequent minima in the r-f voltage. Nonzero minima in the r-f voltage vs. distance correspond to backward-wave amplifier operation.

The results of the above calculations give the operating efficiency and necessary device length CN as functions of the design parameters, including the stream current I_o. The theoretical predictions of efficiency agree well with published experimental data.

LIST OF ILLUSTRATIONS

ANALYSIS OF NONLINEAR O-TYPE BACKWARD-WAVE OSCILLATORS*

INTRODUCTION

The O-type backward-wave oscillator, or O-type carcinotron as it is called by the French, was introduced in 1952 by Kompfner and Williams[1] and has been analyzed extensively for small-signal conditions by many authors. A representative bibliography is given at the end of this report.

The O-type backward-wave oscillator is characterized by its moderate efficiency and its wide electronic tuning range as compared to that of the reflex klystron. The slow-wave structures used are usually either of the helical-waveguide, folded-line or interdigital-line type. A static magnetic field colinear with the direction of r-f propagation is usually used to maintain the electron stream cross section under the influence of space-charge debunching forces.

The operation of the backward-wave oscillator depends upon the interaction of an electron stream with an electromagnetic wave whose phase velocity is in the direction of the electron motion and whose group velocity is oppositely directed. Periodic r-f structures such as those cited above support many modes of propagation, some of which have oppositely directed phase and group velocities. The interaction process in the backward-wave device is essentially that of the forward-wave device in that an r-f signal impressed on the circuit or produced by noise in the electron stream velocity

---

* Presented at the Symposium on Electronic Waveguides, Polytechnic Institute of Brooklyn, April 8, 9 & 10, 1958.

1. See reference 7.

modulates the stream, which in turn produces a density modulation which induces an r-f field onto the circuit in such a way as to add to the existing circuit field. The induced wave will then travel along the circuit with a phase velocity approximately equal to the electron velocity. The wave energy or group velocity traveling opposite to the electron flow produces additional bunching, which in turn produces an increased energy on the circuit, resulting in regenerative amplification for extremely small stream currents and unstable regeneration or oscillation at higher stream currents provided that other necessary oscillation conditions are satisfied.

Thus backward-wave devices, both oscillators and amplifiers, will be inherently less efficient than forward-wave amplifiers of the same type, since in the forward-wave amplifier the density modulation in the stream and the circuit field producing it travel in the same direction, whereas in the backward-wave device they travel in opposite directions, which results in the circuit field being strongest where the modulation is weakest and vice versa. It should be recalled that this backward traveling wave is not a reflected wave from the output transducer but is a property of the mode of operation of the circuit. Reflected waves from the output or from the attenuator in the forward-wave amplifier do not velocity-modulate the stream and lead to electronically tunable oscillation because the reflected-wave phase velocity is opposite to the electron velocity.

The circuit fields and the r-f current in the stream as a function of distance are shown in Fig. 1 for both forward-wave amplifiers and backward-wave oscillators. In the forward-wave device it is seen that the circuit voltage grows at an exponential rate until the nonlinear regime is reached and finally the circuit voltage achieves a saturation value. As would be

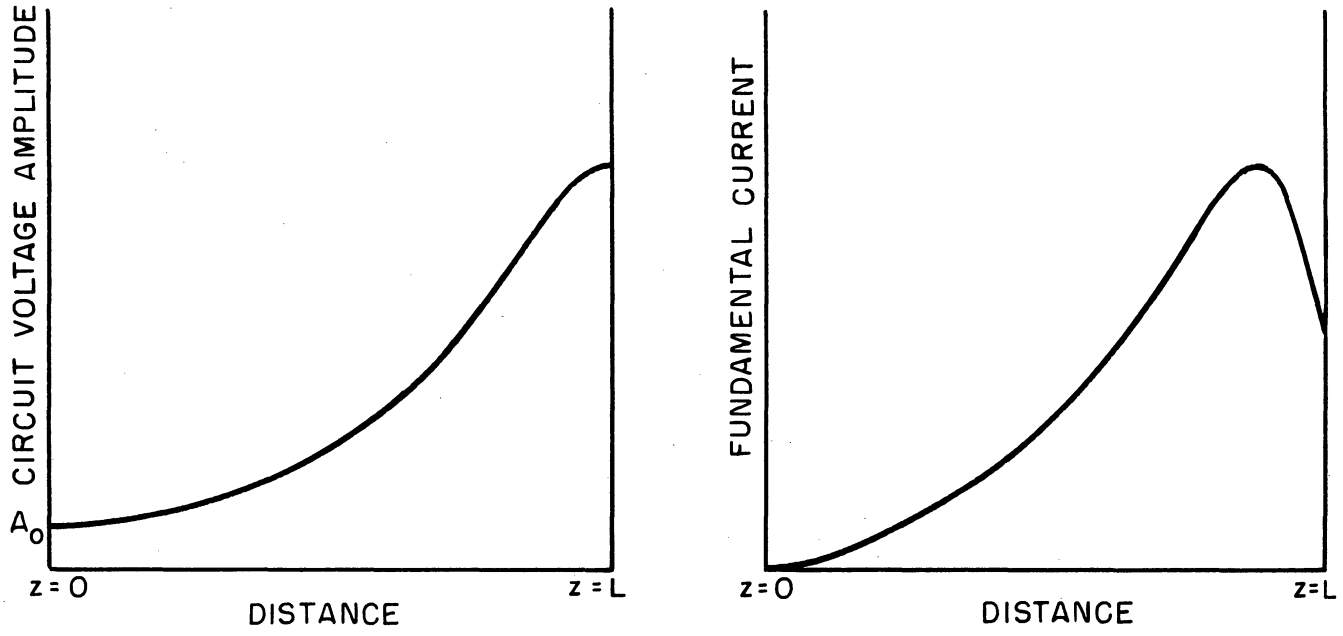

a. NONLINEAR FORWARD-WAVE AMPLIFIER.

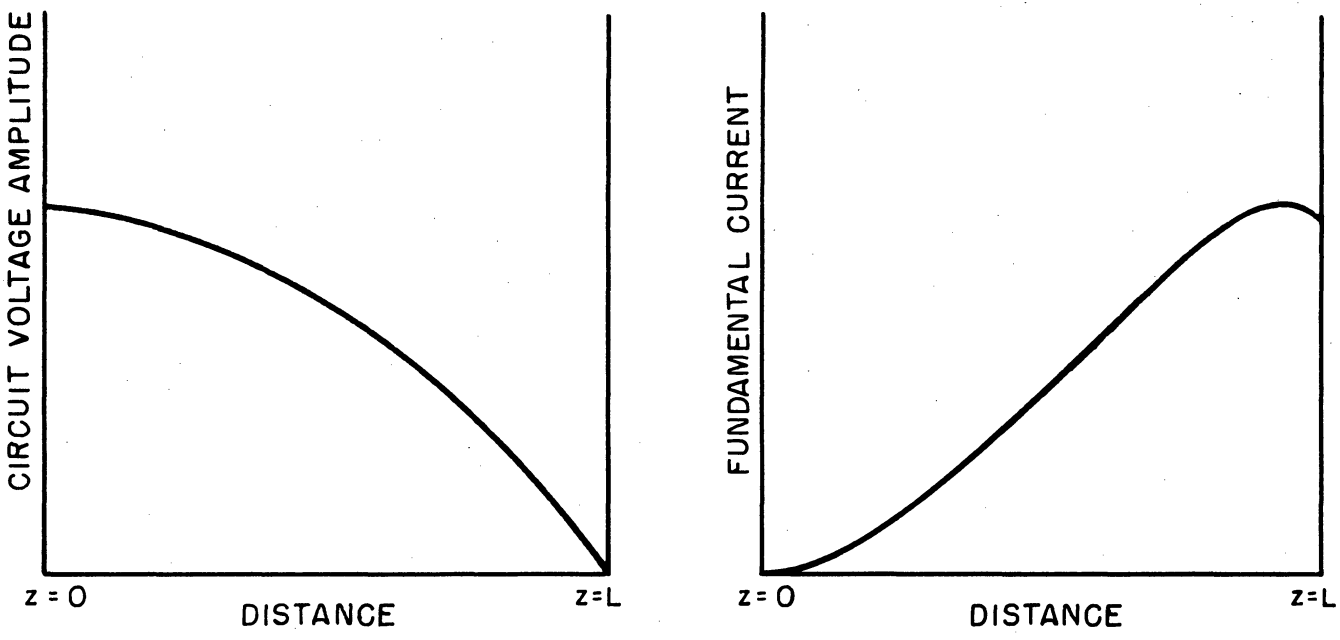

b. NONLINEAR BACKWARD-WAVE OSCILLATOR.

FIG. 1 CIRCUIT VOLTAGE AND FUNDAMENTAL STREAM CURRENT IN FORWARD- AND BACKWARD-WAVE DEVICES.

expected, the fundamental component of current in the stream reaches a maximum approximately a quarter circuit wavelength before the circuit voltage reaches its maximum. In the backward-wave device the circuit voltage falls off approximately as a cosine function and eventually goes through zero with an oscillation condition or reaches a nonzero minimum value in the case of a backward-wave amplifier. The fundamental current in the stream may reach a maximum before the end of the device, i.e., the length for infinite gain, at the critical length or may still be increasing at the critical length depending upon the level of oscillation.

External feedback paths applied to forward-wave amplifiers can produce unstable regenerative amplification, but it is usually characterized by mode instability which results in a discontinuous tuning curve. In both the amplifier and the oscillator the interaction is between the slow space-charge wave of the stream and the circuit wave. In fact, under usual conditions in the oscillator the fast space-charge wave is excited to a negligible extent.

A considerable amount of theoretical work has been done on backward-wave oscillators using the modified linear forward-wave amplifier theory and neglecting the effects of space charge or large C or both. Some work by Grow and Watkins[2] has incorporated both of these effects into the linear theory and then made estimates of the efficiency assuming specific values for the ratio of fundamental r-f current to the d-c current in the stream. Recently Sedin[3] reported on some nonlinear calculations pertaining to the backward-wave oscillator where he used Nordsieck's[4] equations, suitably modified and neglecting the effects of finite C, QC and circuit loss.

---

2. See reference 3.

3. See reference 13.

4. See reference 9.

It is one of the objectives of this report to present the large-C space-charge linear equations for backward-wave amplifiers and oscillators and to discuss interesting facets of their solutions. The second purpose of this report is to derive the equations and discuss the solutions of the non-linear backward-wave device equations including the effects of finite C, space charge and circuit loss. The derived equations apply equally well to both the backward-wave amplifier and the oscillator. It is anticipated that the results will be useful in understanding the limitations and possibilities inherent in backward-wave devices. Efficiency considerations are important in backward-wave devices and it is useful to know the theoretical limit and what factors need be optimized to achieve this plateau. The linear equations give information also on the dependence of the propagation constants and the gain of backward-wave amplifiers on circuit and stream parameters.

BACKWARD-WAVE CIRCUITS

In backward-wave interaction as well as in forward-wave interaction it is required that the circuit wave and the electron stream be in approximate synchronism. This requirement results in a voltage-tunable device in the case of backward-wave interaction, since the r-f circuit must be dispersive in order to obtain oppositely directed phase and group velocities. The phase and group velocities of periodic structures are written as

$$v_p = \frac{\omega}{\beta} \tag{1}$$

and

$$v_g = \frac{v_p}{1 - \frac{\omega}{v_p}\frac{dv_p}{d\omega}} \tag{2}$$

A negative group velocity requires that the circuit exhibit negative dispersion; i.e., the denominator must remain negative.

Any r-f propagating circuit that satisfies the requirement of oppositely directed phase and group velocities for at least one space harmonic component of the total field can be used as a backward-wave device circuit. These space harmonics exist in all periodic structures, as indicated by the periodic nature of the boundary conditions. The fields can be expressed over all periods of the r-f structure in terms of their values over one period through the use of Floquet's theorem. As mentioned earlier in the report, helical waveguides and interdigital lines have found most wide application in oscillators of the O-type. Interdigital lines and vane-type structures are frequently used in M-type backward-wave oscillators.

It is well known that these circuits can be represented by an equivalent circuit in the form of an L-C transmission line (low-pass filter) when operating in the fundamental forward-wave mode. In this embodiment of the equivalent circuit the inductance and any series circuit loss are represented by the series elements and the capacitance by a shunt element. The equation for the voltage along the line as a function of distance and time is a linear second-order partial differential equation containing driving terms when an electron stream is present. It is known that this type of circuit has a phase shift per section which increases with frequency due to the series inductance. In the nondispersive region where it is usually operated the phase velocity is independent of frequency and is given by $v_o = 1/\sqrt{LC}$.

Usually the differential equation for the circuit voltage in a backward-wave device is found by simply changing the sign of the circuit impedance to account for backward energy flow. The equivalent circuit may be

drawn by interchanging the positions of the series inductance and the shunt capacitance to give a high-pass type of circuit with a phase shift per section characteristic which decreases with frequency. The phase velocity for this circuit is an increasing function of frequency and is given by $v_o = -\omega^2\sqrt{LC}$. A differential equation of fourth order in time and second order in the distance for the voltage along the line can be derived for this circuit. This equation can be reduced to a second-order equation if a time variation of exp $j\omega t$ is introduced. The presence of an electron stream also adds driving terms to the circuit equation.

The forms of the two equivalent circuits are shown in Fig. 2 and the differential equation used both for the nonlinear forward-wave amplifier and for the backward-wave device is given below. In those terms preceded by a double sign the upper sign refers to the forward-wave device and the lower sign to the backward-wave device. The backward-wave device equations apply equally well to the oscillator and the amplifier.

$$\frac{\partial^2 V(z,t)}{\partial t^2} - v_o^2 \frac{\partial^2 V(z,t)}{\partial z^2} + 2\omega Cd \frac{\partial V(z,t)}{\partial t} = \pm v_o Z_o \frac{\partial^2 \rho(z,t)}{\partial t^2}$$

$$\pm 2\omega C d Z_o v_o \frac{\partial \rho(z,t)}{\partial t} . \qquad (3)$$

The symbols used in the above and subsequent equations are defined in a list of symbols at the end of the report. While it is intuitively satisfying the the backward-wave equivalent circuit cannot be realized in terms of a smooth circuit but only in terms of lumped parameters to give the desired, oppositely directed phase and group velocities. This form of the circuit also leads to difficulties in attaching physical significance to the circuit elements. It

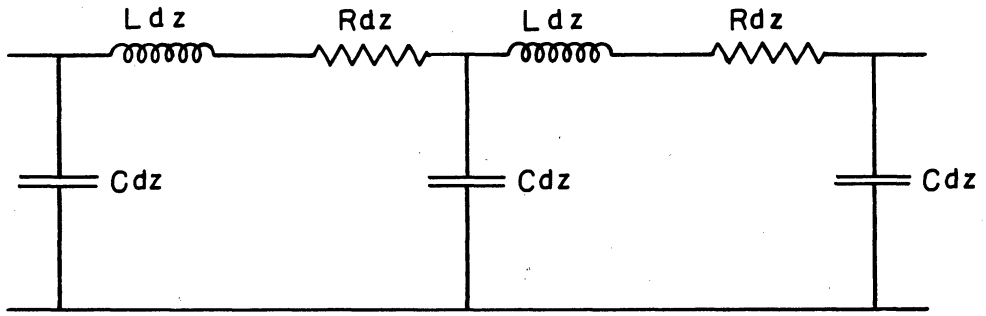

L = HENRYS / METER

R = OHMS / METER

C = FARADS / METER

$$v_o = \frac{1}{\sqrt{LC}}$$

$$z_o = \sqrt{\frac{z}{Y}}$$

a. FORWARD-WAVE CIRCUIT.

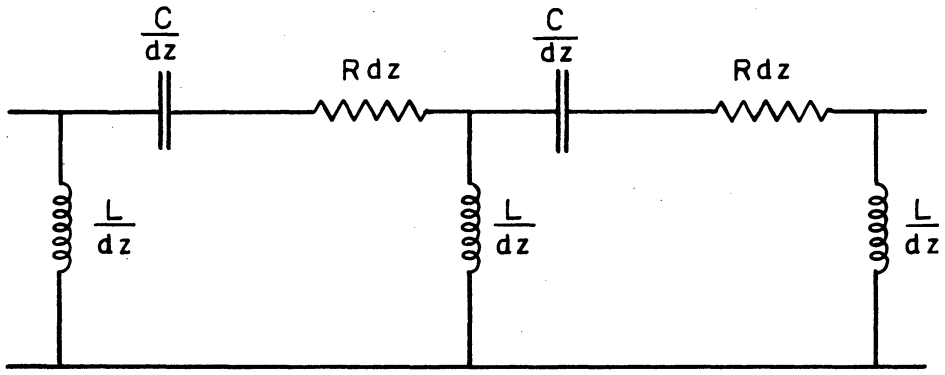

L = HENRYS · METER

R = OHMS / METER

C = FARADS · METER

$$v_o = -\omega^2\sqrt{LC}$$

$$Z_o = \sqrt{\frac{z}{Y}}$$

b. BACKWARD-WAVE CIRCUIT.

FIG. 2 EQUIVALENT CIRCUITS FOR FORWARD-WAVE AND BACKWARD-WAVE DEVICES.

is generally most satisfying simply to change the sign of the circuit impedance.

SMALL-SIGNAL BACKWARD-WAVE EQUATIONS

The small-signal backward-wave device equations have been derived by Johnson[5] following the method used by Pierce to derive the forward-wave amplifier equations under the assumptions of negligible C. Johnson defines a circuit impedance $K = -E_z^2/2\beta^2 P$ and a passive mode parameter Q which is the negative of Pierce's Q in order to keep QC positive. The total electric field acting on the electron stream is then written as

$$E = \left[\frac{-\Gamma_1\Gamma^2 K}{(\Gamma_1^2 - \Gamma^2)} - \frac{2j\Gamma^2 QK}{\beta_e}\right] i \ , \tag{4}$$

where the two terms on the right-hand side represent the circuit field and the space-charge field acting on the stream. The second term represents the effect of all nonsynchronous and passive modes and this component of the field cannot be coupled out to the circuit. Its effect is greatest when the space charge is strongest. From Johnson's work the propagation constants in the presence and absence of the stream are defined as

$$-\Gamma \triangleq -j\beta_e + \beta_e C\delta \tag{5}$$

$$-\Gamma_1 \triangleq -j\beta_e - j\beta_e Cb + \beta_e Cd \ . \tag{6}$$

---

5. See reference 6.

The next step in the derivation of the linear backward-wave device equations is to substitute the above expressions for the propagation constants into the field equation and simplify.

If this is done and all terms are retained, rather than neglecting terms of the order of C as Johnson did, the following quartic determinantal equation is obtained.

$$\delta^2 = \frac{(1 + jC\delta)^2 [1 + C(b \mp jd)]}{\left[\mp b + jd \pm j\delta + C\left(jbd \mp \frac{b^2}{2} \pm \frac{d^2}{2} \mp \frac{\delta^2}{2}\right)\right]} - 4\,QC(1 + jC\delta)^2 . \qquad (7)$$

In the terms preceded by double signs the upper sign refers to the forward-wave amplifier and the lower sign to the backward-wave device. Equation 7 reduces to Johnson's cubic equation when terms involving C are neglected. The above equation may be reduced to a cubic by neglecting the wave whose phase velocity is oppositely directed to the direction of the electron stream. For particular values of the parameters C, QC, d and b the solutions of the above equation give the propagation constants of the complete set of waves propagating on the structure. These results are applicable to both the backward-wave amplifier and the backward-wave oscillator.

Typical sets of the backward-wave propagation constants are shown in Figs. 3 and 4 for large C and QC. These were obtained by solving the determinantal equation for the backward-wave device. These backward-wave propagation constants look very much like the forward-wave propagation constants for negative b values. When C is small the backward-wave propagation constants can in fact be found from the forward-wave propagation constants by using the appropriate transformation. The backward-wave propagation constants are seen to be mirrored about both the b and x, y axes with respect to the forward-wave propagation constants. For large C this transformation does not hold

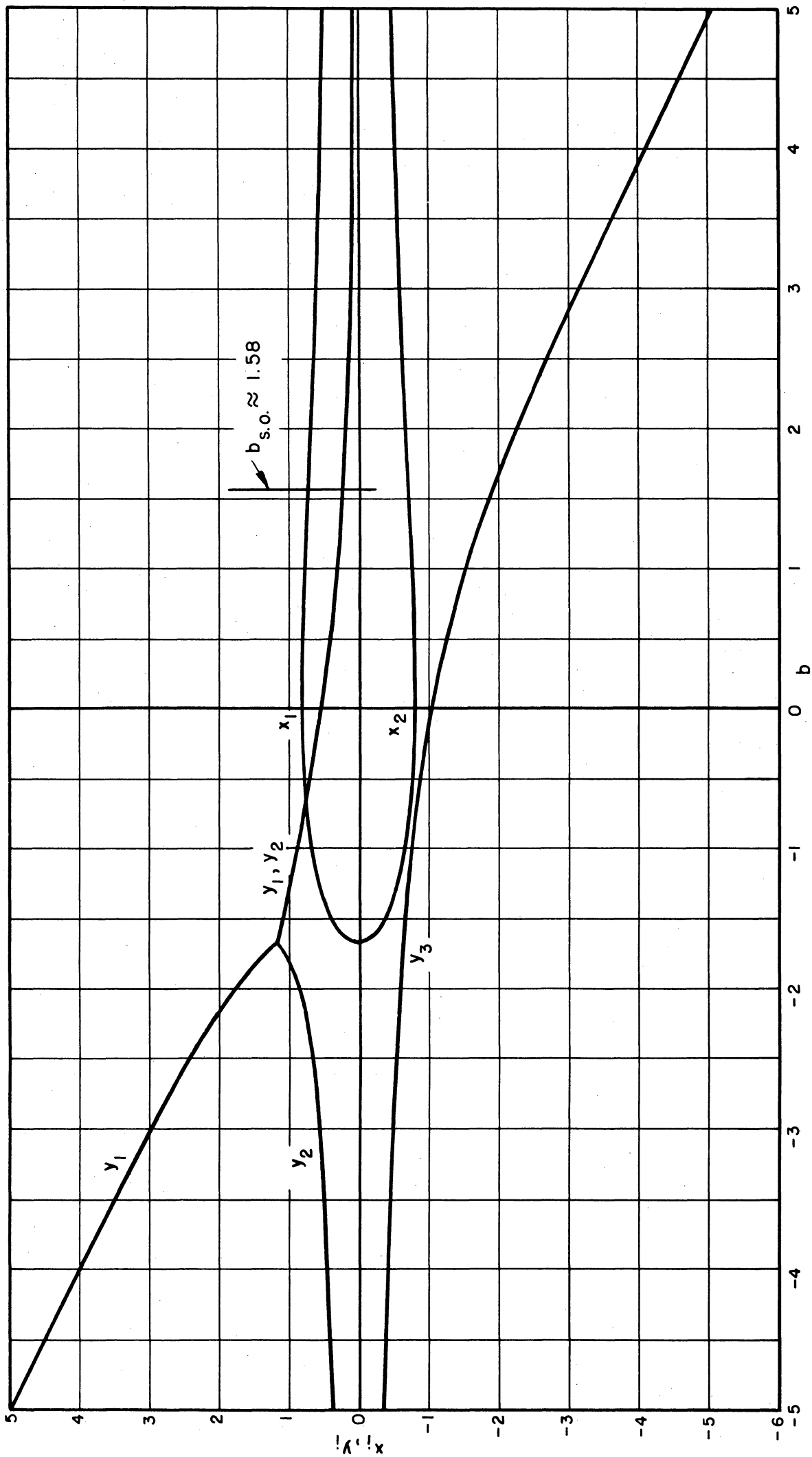

FIG. 3 BACKWARD-WAVE PROPAGATION CONSTANTS. (C = 0.1, QC = 0, d = 0)

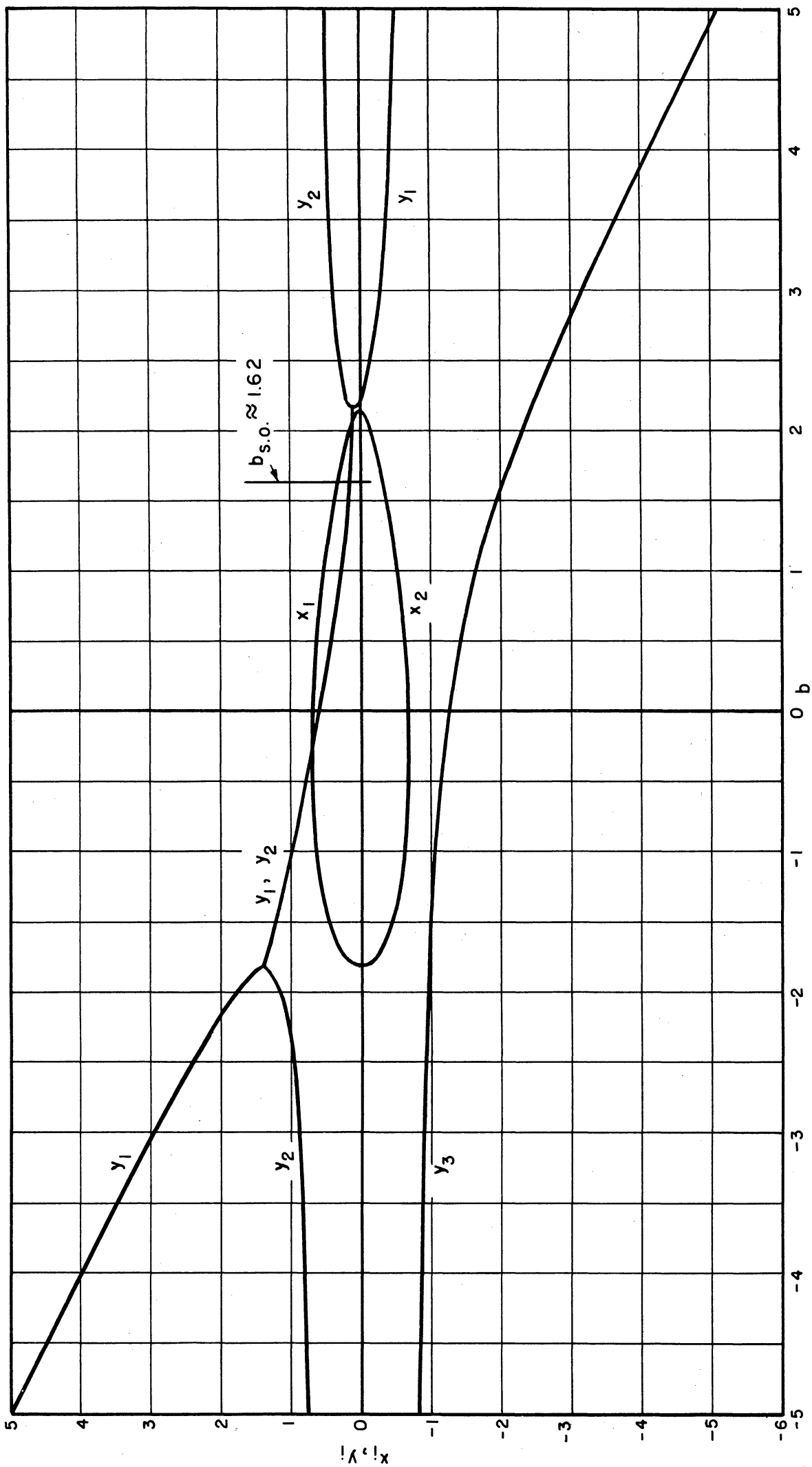

FIG. 4 BACKWARD-WAVE PROPAGATION CONSTANTS. (C = 0.1, QC = 0.125, d = 0)

and the roots must be obtained directly from the backward-wave determinantal equation. When QC is zero the propagation constants remain complex for very large values of b and the propagation constants are consequently complex for the oscillation condition. As QC is increased from zero the point at which the propagation constants become pure imaginary occurs at lower values of b and it is found that the propagation constants are pure imaginary at the start oscillation condition for QC > 0.15. In the case of the backward-wave amplifier the optimum value of b is near zero even for large values of C and QC. The value of b that leads to an oscillation condition cannot be determined from these plots alone but must be determined by combining the determinantal equation with the equation expressing the circuit voltage as a function of distance.

The r-f voltage along the structure may be written in terms of the amplitudes of the three waves as

$$\frac{V_z}{V} = e^{-j\frac{\theta}{C}} \sum_{i=1}^{3} \left(\frac{V_i}{V}\right)\left(\frac{V_{ci}}{V_i}\right) e^{\delta_i \theta} , \qquad (8)$$

where $\theta \triangleq 2\pi CN$,

V_i = r-f voltage amplitude of the wave,

V_{ci} = circuit component of wave voltage, and

V = total voltage at $z = 0$.

If it is assumed that an unmodulated electron stream is injected at $z = 0$ and that the circuit voltage may be represented as the sum of three circuit voltages at the input, the following relations are determined.

$$\sum_{i=1}^{3} \frac{(1 + jC\delta_i)\, V_i}{\delta_i} = \left(\frac{ju_oC}{\eta}\right)\tilde{v} , \tag{9}$$

$$\sum_{i=1}^{3} \frac{(1 + jC\delta_i)\, V_i}{\delta_i^2} = \left(\frac{-2V_oC^2}{I_o}\right)\tilde{i} , \tag{10}$$

$$V = V_1 + V_2 + V_3$$

and

$$V_c = V_{c1} + V_{c2} + V_{c3} , \tag{11}$$

where $\tilde{v}$ and $\tilde{i}$ are respectively r-f velocity and convection current. Equations 9, 10 and 11 are solved simultaneously to give the normalized amplitudes of the individual waves. The general result is shown below.

$$\frac{V_i}{V} = \left[1 + \frac{1 + jC\delta_i}{1 + jC\delta_{i+1}}\left(\frac{\delta_{i+1}}{\delta_i}\right)^2 \frac{\delta_{i+2} - \delta_i}{\delta_{i+1} - \delta_{i+2}} + \frac{1 + jC\delta_i}{1 + jC\delta_{i+2}}\left(\frac{\delta_{i+2}}{\delta_i}\right)^2 \frac{\delta_i - \delta_{i+1}}{\delta_{i+1} - \delta_{i+2}}\right]^{-1} , \tag{12}$$

where $\delta_i \equiv \delta_{i+3}$.

The above equation gives the total voltage associated with each wave and in the absence of space charge gives the circuit voltage. It was mentioned earlier that the effect of space charge is to reduce the circuit component of voltage and this reduction is found from the ratio of the second term on the right-hand side of the determinantal equation to the total right-hand side of this equation. The result is

$$\frac{V_{ci}}{V_i} = 1 + 4QC\,\frac{(1 + jC\delta_i)^2}{\delta_i^2} , \tag{13}$$

where $\delta_i \equiv \delta_{i+3}$. It is easily shown that Eqs. 12 and 13 are the same for both forward-wave and backward-wave devices.

In the region of b where the wave propagation constants are complex the voltage amplitudes V_{ci}/V are complex, as can be seen from Eqs. 12 and 13. When the propagation constants become pure imaginary the circuit voltage amplitudes become pure real. A typical plot of the individual wave amplitudes vs. b is shown in Fig. 5. It is seen that for large values of b the amplitudes of the first and second waves become negligible and the third wave dominates. At the start-oscillation b the amplitude of the second wave is negligible for large QC.

To determine the start-oscillation conditions for the backward-wave oscillator, the backward-wave propagation constants for a given set of C, QC, d and b are found from Eq. 7. Then these propagation constants are substituted into the circuit-voltage equation (8) and certain of these values will result in the circuit voltage V_z/V becoming zero at a particular CN. These values of b and CN are the oscillation conditions. Knowing the structure impedance then permits the calculation of the necessary start-oscillation current, the structure length and the voltage tuning curve. Johnson[6] has tabulated these start-oscillation conditions for very small C as a function of space charge.

There will be many combinations of CN and b which make V_z/V equal to zero for a particular C, QC and d. The lowest-order start-oscillation condition corresponds to the smallest values of b and CN for which $V_z/V = 0$. Higher values correspond to spurious oscillations and for a given tube length

---

6. See reference 6.

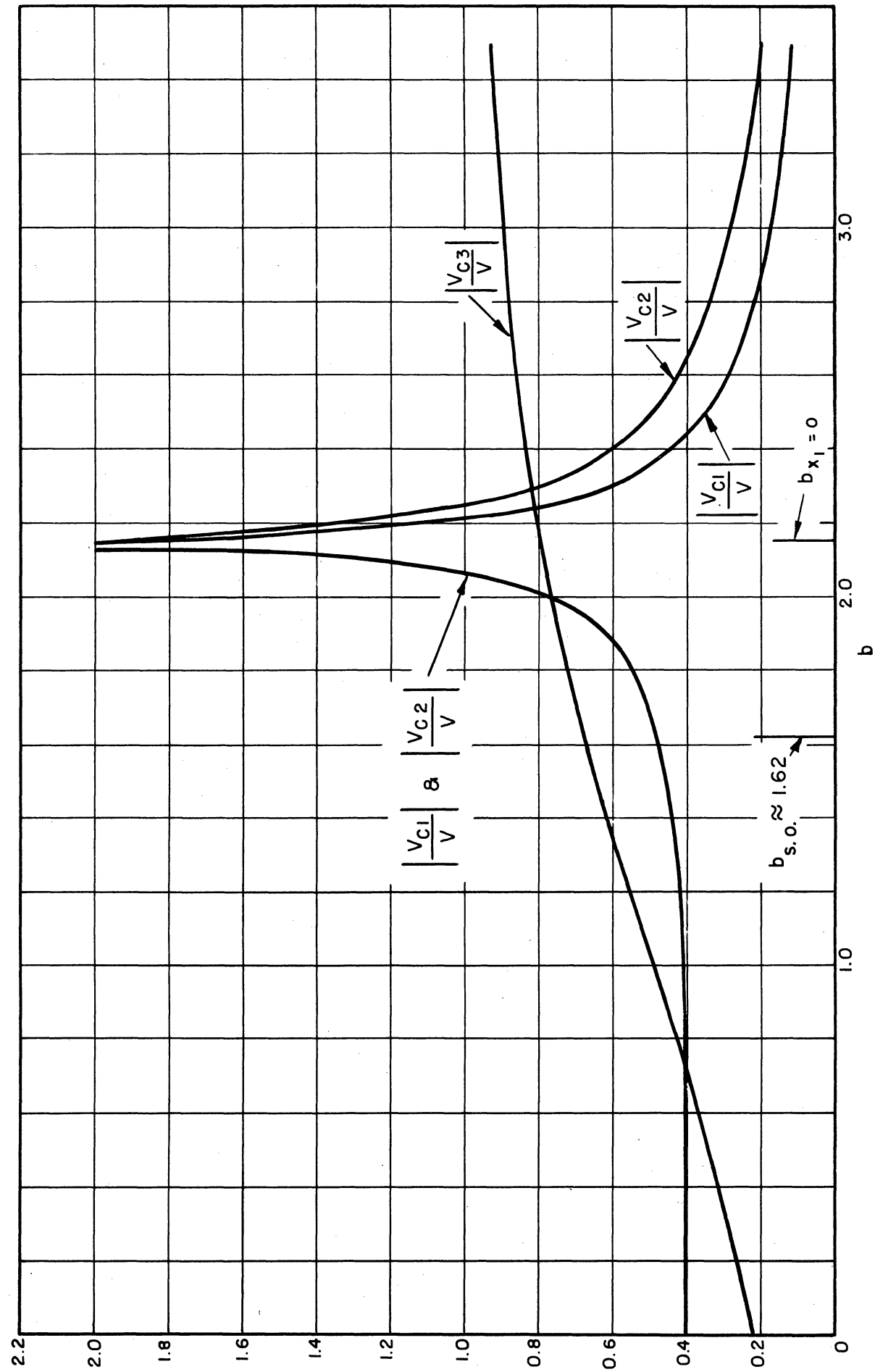

FIG. 5 NORMALIZED WAVE AMPLITUDES VS. b. (C = 0.1, QC = 0.125, d = 0)

describe oscillations at high values of stream current.

It is interesting to plot, for a particular C, QC and d, constant-negative-gain contours on a plot of b vs. the radian tube length $\theta = 2\pi CN$. Such a plot is shown in Fig. 6 for C = 0.10, QC = 0.125, and d = 0. Several possible oscillation conditions are seen on this plot and it is also apparent that the value of b for higher-order oscillations increases with increasing CN and becomes asymptotic to a particular b value. As QC is increased it has been determined that the increase in b for the higher-order oscillations is at a slower rate.

For this same set of operating parameters a plot of gain vs. CN is shown in Fig. 7 for particular values of b. The positive gain values represent attenuation of the circuit wave traveling from right to left in the diagram, i.e., traveling from the collector end to the gun end of the tube. At positive values of b greater than that for which the first wave-growth constant x_1 goes to zero, the wave amplitudes at the gun end of the device are purely real and either in phase or 180 degrees out of phase with respect to one another. Under these conditions the three waves travel with constant amplitudes and different phase velocities along the r-f structure and gain is produced due to a beating between the three waves. This gain is maximum just to the right of the point where x_1 becomes zero. This type of gain can also be shown to exist in forward-wave devices.

NONLINEAR BACKWARD-WAVE EQUATIONS

In this section the nonlinear backward-wave device equations will be presented rather than derived since they can be developed in a simple

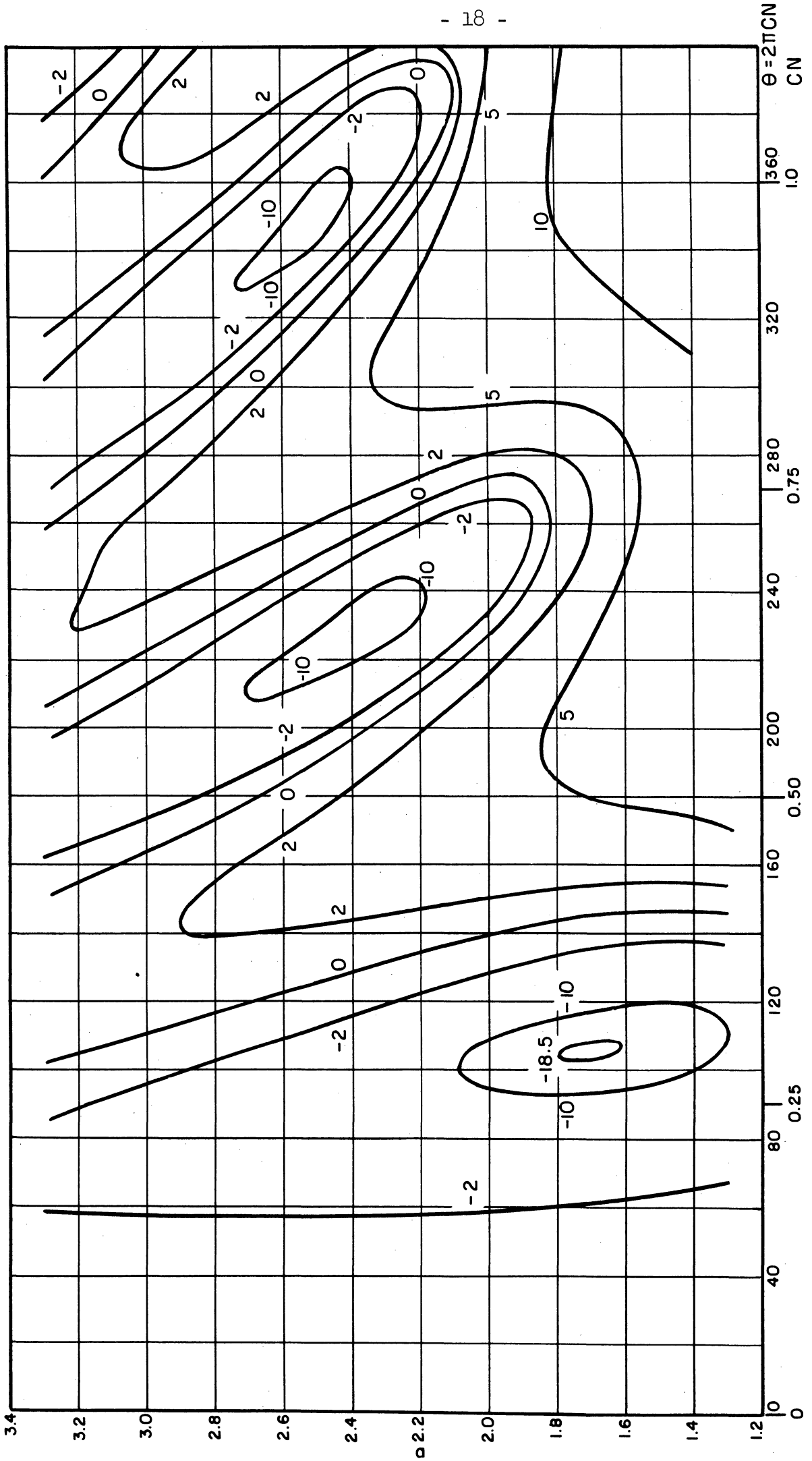

FIG. 6 BACKWARD-WAVE CONSTANT-GAIN CONTOURS. (C=0.1, QC=0.125, d=0)

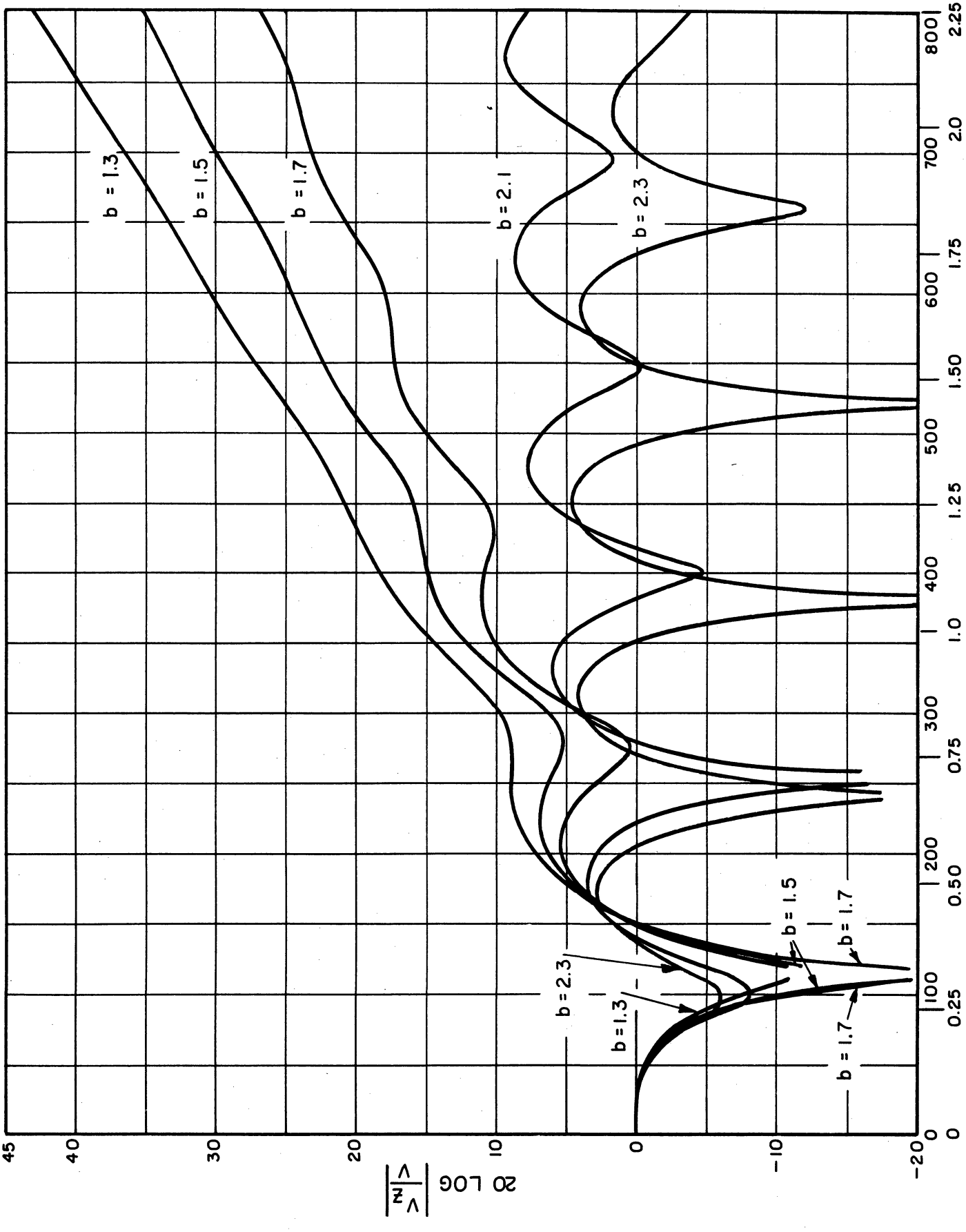

FIG. 7 GAIN VS. LENGTH IN A BACKWARD-WAVE DEVICE. ($C = 0.05$, $QC = 0.125$, $d = 0$, $b_{s.o.} \approx 1.6$)

manner from the nonlinear forward-wave amplifier equations[7]. The circuit equation used for the nonlinear backward-wave analysis is that given in Eq. 3 with the lower signs. The normalized variables used in the analysis are defined below.

$$y \triangleq \frac{C\omega z}{u_o} = 2\pi C N_s \tag{14}$$

$$\phi_o \triangleq \omega t_o \tag{15}$$

$$\theta(y) \triangleq \frac{y}{C} - \omega t - \phi(y,\phi_o) \tag{16}$$

$$u_t(y,\phi_o) \triangleq u_o\left[1 + 2Cu(y,\phi_o)\right] \tag{17}$$

$$V(y,\phi) \triangleq \mathrm{Re}\left[\frac{Z_o I_o}{C} A(y)\, e^{-j\phi}\right] \tag{18}$$

Following a procedure similar to that used in obtaining the forward-wave equations the following set of working equations is obtained for backward-wave O-type devices.

$$\frac{\partial\phi(y,\phi_o)}{\partial y} + \frac{d\theta(y)}{dy} = \frac{2u(y,\phi_o)}{1 + 2Cu(y,\phi_o)}\,, \tag{19}$$

---

7. See reference 12.

$$\frac{d^2A(y)}{dy^2} - A(y)\left[\left(\frac{1}{C} - \frac{d\theta(y)}{dy}\right)^2 - \frac{(1+Cb)^2}{C^2}\right] = \pm \frac{(1+Cb)}{\pi C}\left[\int_0^{2\pi} \frac{\cos \phi(y,\phi_o')\, d\phi_o'}{1 + 2Cu(y,\phi_o')}\right.$$

$$\left. + 2Cd \int_0^{2\pi} \frac{\sin \phi(y,\phi_o')\, d\phi_o'}{1 + 2Cu(y,\phi_o')}\right] , \quad (20)$$

$$A(y)\left[\frac{d^2\theta(y)}{dy^2} - \frac{2d}{C}(1+Cb)^2\right] + 2\frac{dA(y)}{dy}\left(\frac{d\theta(y)}{dy} - \frac{1}{C}\right)$$

$$= \pm \frac{(1+Cb)}{\pi C}\left[\int_0^{2\pi} \frac{\sin \phi(y,\phi_o')\, d\phi_o'}{1 + 2Cu(y,\phi_o')}\right.$$

$$\left. - 2Cd \int_0^{2\pi} \frac{\cos \phi(y,\phi_o')\, d\phi_o'}{1 + 2Cu(y,\phi_o')}\right] , \quad (21)$$

and

$$\frac{\partial u(y,\phi_o)}{\partial y}\left[1 + 2Cu(y,\phi_o)\right] = A(y)\left[1 - C\frac{d\theta(y)}{dy}\right] \sin \phi(y,\phi_o)$$

$$- C\frac{dA(y)}{dy} \cos \phi(y,\phi_o) - \frac{1}{1+Cb}\left(\frac{\omega_p}{\omega C}\right)^2 \int_0^{2\pi} \frac{F(\phi-\phi')\, d\phi_o'}{1 + 2Cu(y,\phi_o')} . \quad (22)$$

The independent variables appearing in the equations are y, the distance along the tube in normalized units, and the entrance phase ϕ_o of the electrons

relative to the r-f wave at the input to the tube. The dependent variables are A(y), the normalized r-f voltage amplitude along the structure; $\theta(y)$, the phase lag across the amplifier at any y; $\phi(y,\phi_o)$, the phase of the displacement component of an electron that entered the helix at the moment ϕ_o relative to the r-f wave; and $u(y,\phi_o)$, the a-c velocity parameter of an electron at any point y.

The upper signs preceding the terms on the right-hand side of Eqs. 20 and 21 refer to the forward-wave device and the lower signs refer to the backward-wave device.

The assumptions made in the derivation of the above equations are:

1. The electric field, electron velocity and current are assumed to be functions only of distance along the tube and time and not functions of the radial dimension.

2. A solid model of the electron stream is assumed in developing the space-charge field expression. The equivalence of this method and the method used by Tien and Walker in obtaining a space-charge field expression can be shown.

3. The structure impedance is assumed to be only at the fundamental backward space harmonic.

4. Rectilinear electron flow is assumed so that the electrons have no transverse motion.

5. Nonrelativistic mechanics is used.

The boundary conditions to be used in the nonlinear backward-wave device analysis are very similar to those used in solving the forward-wave amplifier equations. The r-f structure is assumed to be matched to its characteristic impedance over its entire length and the problem is handled as an initial value problem rather than a boundary value problem. The dependent variables and their derivatives are specified at the input boundary and the equations then integrated until a minimum in the r-f voltage is

reached as a function of distance. It is assumed that the electron stream enters the interaction region in an unmodulated state so that all the electrons at y = 0 have a zero a-c velocity and the same average velocity. The electrons are assumed to enter equally spaced over one period of the r-f wave at the input; therefore their initial phase positions are given. An initial value A_o of the r-f signal is assumed and if there is no circuit loss, $dA(y)/dy$ at the input is zero. The initial phase lag is of course zero and its derivative $d\theta(y)/dy$, the apparent phase constant of the total wave at the input, is found from the small-signal solutions as in the forward-wave amplifier theory.

The nonlinear backward equations can be solved by assuming specific values of the injection velocity b and the amplitude of the circuit voltage at y = 0 (A_o) for any set of C, QC and d. Then the equations are integrated numerically using the appropriate difference equation formulation consistent with accuracy and stability of the system until the circuit voltage goes through a minimum in the case of a backward-wave amplifier or goes through zero in the case of an oscillator. The number of representative electrons which have to be used in finding the solutions depends critically upon the value of the space-charge parameter, increasing as QC becomes quite large (around 0.5). As the collector end of the tube is approached, i.e., as the circuit field becomes very small, electrons begin to overtake one another and a maximum in the fundamental component of stream current is reached as in the forward-wave amplifier.

It is apparent that in a backward-wave oscillator that is relatively short (CN approximately 0.3) the effect of crossing electron flight lines is not as important as in the forward-wave amplifier where the typical circuit

lengths are quite great, since crossing occurs first in a backward-wave oscillator very near the collector end where the circuit voltage is small and decreasing approximately as a cosine function. Overtaking of electrons does not result in an abrupt change in the slope of the voltage vs. distance curve. Of course in the backward-wave amplifier where long structures would be used overtaking of electrons, resulting in multi-valued velocities, would be important as in the forward-wave amplifier. In the event that electron trajectory crossings are not of great importance the Eulerian formulation of the equations could be used and hence the hydrodynamical form of the continuity equation is appropriate. This would result in a somewhat simpler set of equations to be solved and the effects of space charge could be more easily included.

In order to determine the combination of b and CN that leads to an oscillation condition several trials are required. The sensitivity of the start-oscillation conditions to the value of A_o at constant b for a particular set of C, QC and d is shown in Fig. 8, where oscillation occurred for A_o equal to 0.68 and 0.685 but not for 0.67 and 0.69.

A detailed study of the variation of the phase lag across the amplifier $\theta(y)$ vs. y is useful in determining the direction of the change necessary in b or A_o when in the neighborhood of an oscillation condition. The behavior of $\theta(y)$ in the neighborhood of an oscillation condition is illustrated in Fig. 9. This dependence is general for any set of circuit and stream parameters. It is seen that a nearly linear relationship of $\theta(y)$ vs. y is obtained at the oscillation condition. This is also true when the values of b and A_o are far from a start-oscillation condition and hence one must be

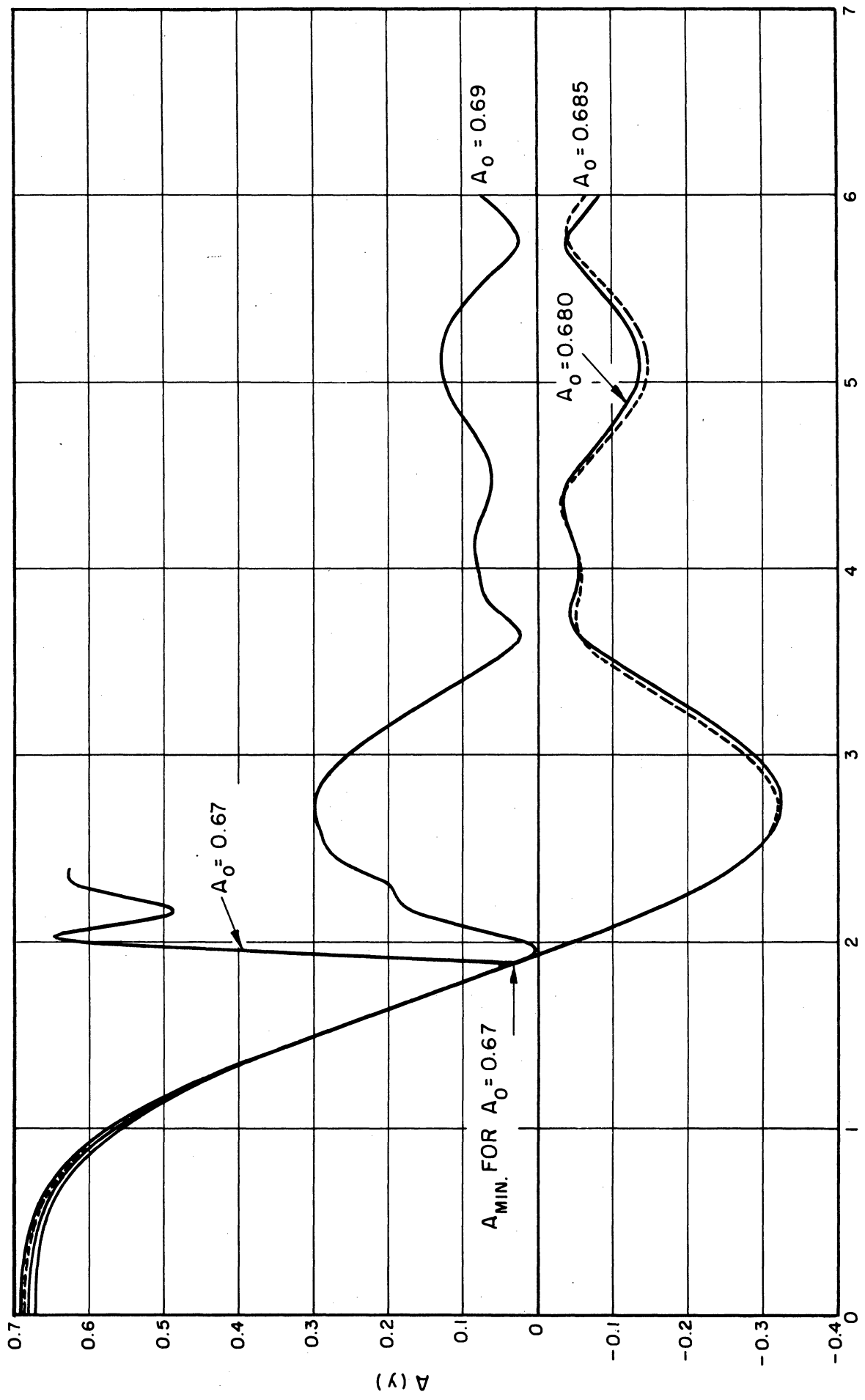

FIG. 8 R-F VOLTAGE AMPLITUDE VS. DISTANCE. (C = 0.1, QC = 0, d = 0, b = 1.9)

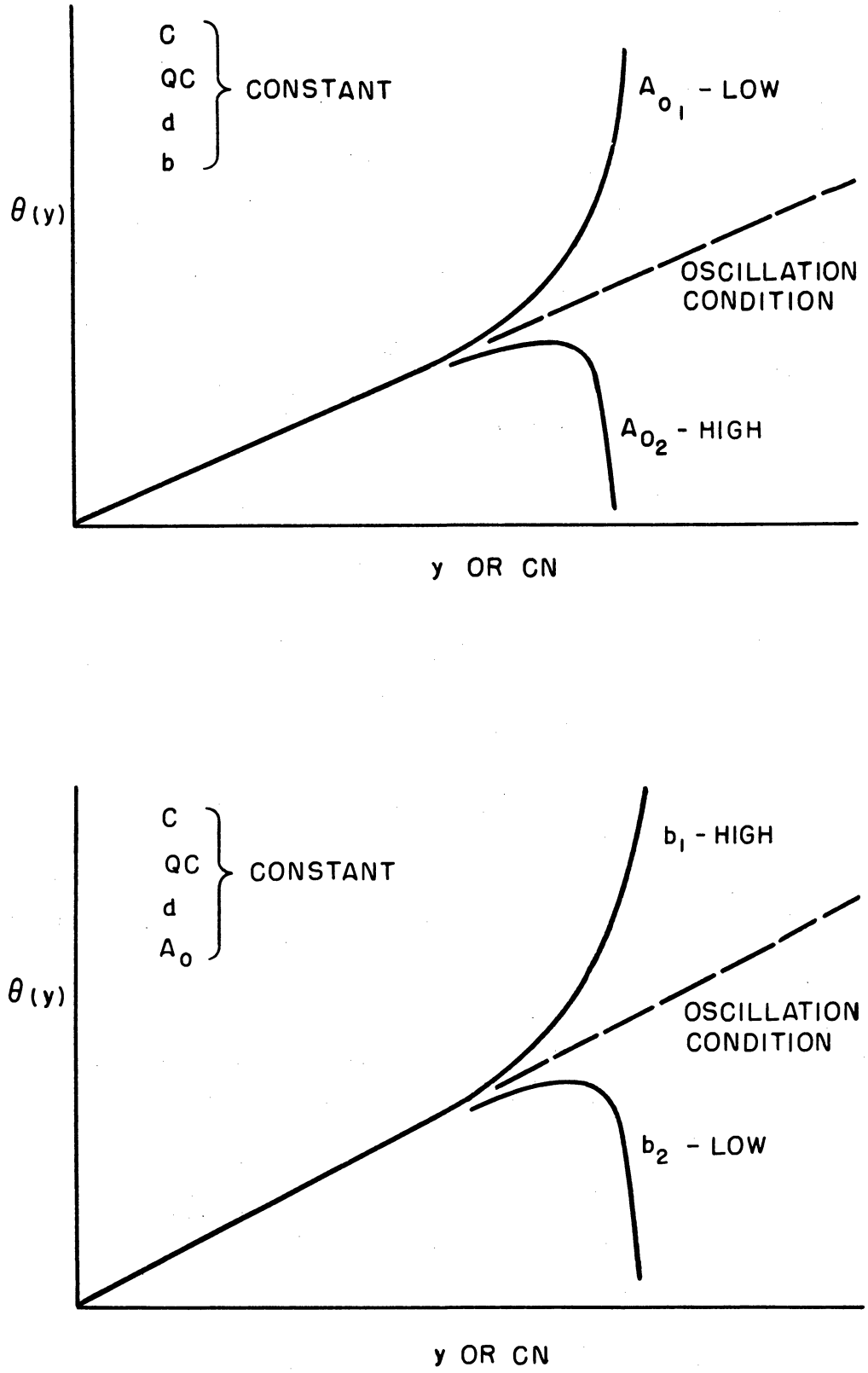

FIG. 9 INDICATION OF PROXIMITY TO AN OSCILLATION CONDITION.

near the optimum combination of b and A_o to use the criterion illustrated in the above figure. As the ratio of stream current to minimum starting current is increased, the oscillation condition is more difficult to locate and it is necessary to examine a plot of the CN to the minimum value of A(y) vs. A_o as well as the above plot in order to determine the oscillation conditions.

EFFICIENCY CALCULATIONS

The CN length and value of b required for lowest-order start-oscillation condition may be determined by assuming an arbitrarily small value of the signal level A_o at z = 0 and then varying b for any particular set of C, QC and d. A plot of the CN_s for this lowest-order oscillation, which corresponds to minimum starting current, and the value of the injection velocity parameter required is shown in Fig. 10. The required length and value of b are seen to decrease as the space charge is increased. The values of QC shown correspond to values of $\omega_q/\omega C$ between 0 and 1.5. These results agree well with those predicted using the linear theory.

As the value of b is increased from that corresponding to the lowest start-oscillation current, larger values of A_o are required to produce oscillation. The efficiency increases approximately linearly with increasing b at constant C, QC and d. The point at which the circuit voltage A(y) goes through zero occurs at a larger value of CN_s in general, which signifies an increase in the stream current above the minimum start-oscillation value. For moderate values of C the length N is nearly independent of the stream current, so that CN varies as the one-third power of the current. If this relationship is true for C's as large as 0.1 the ratio of stream current to

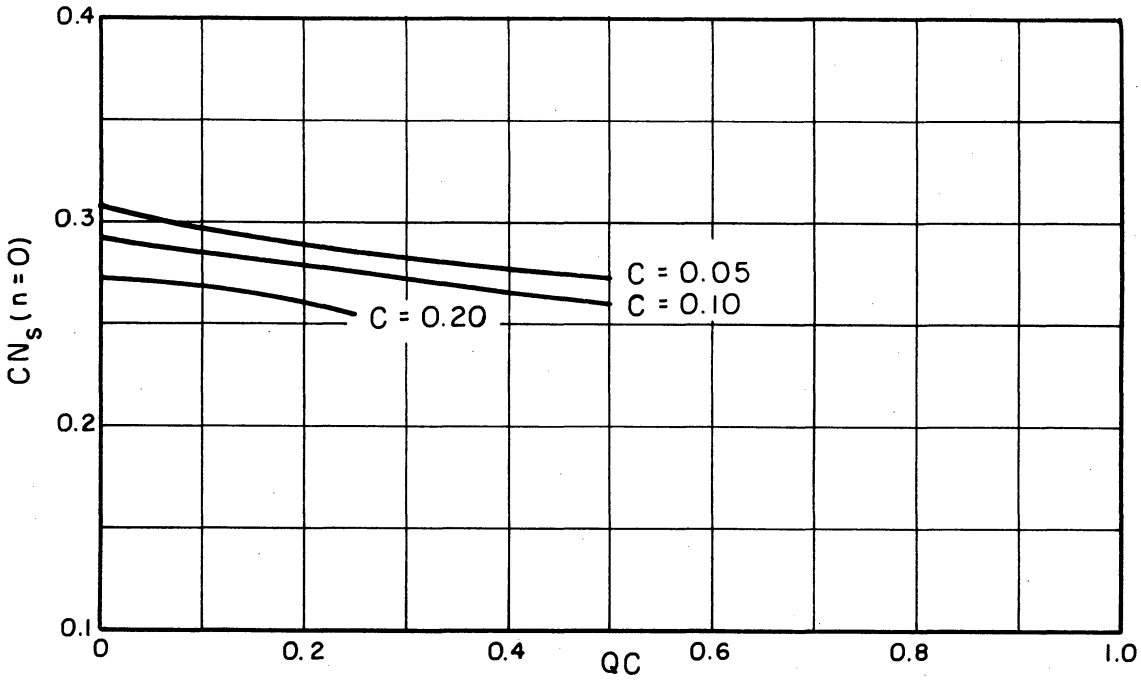

a. CN_s VS. QC.

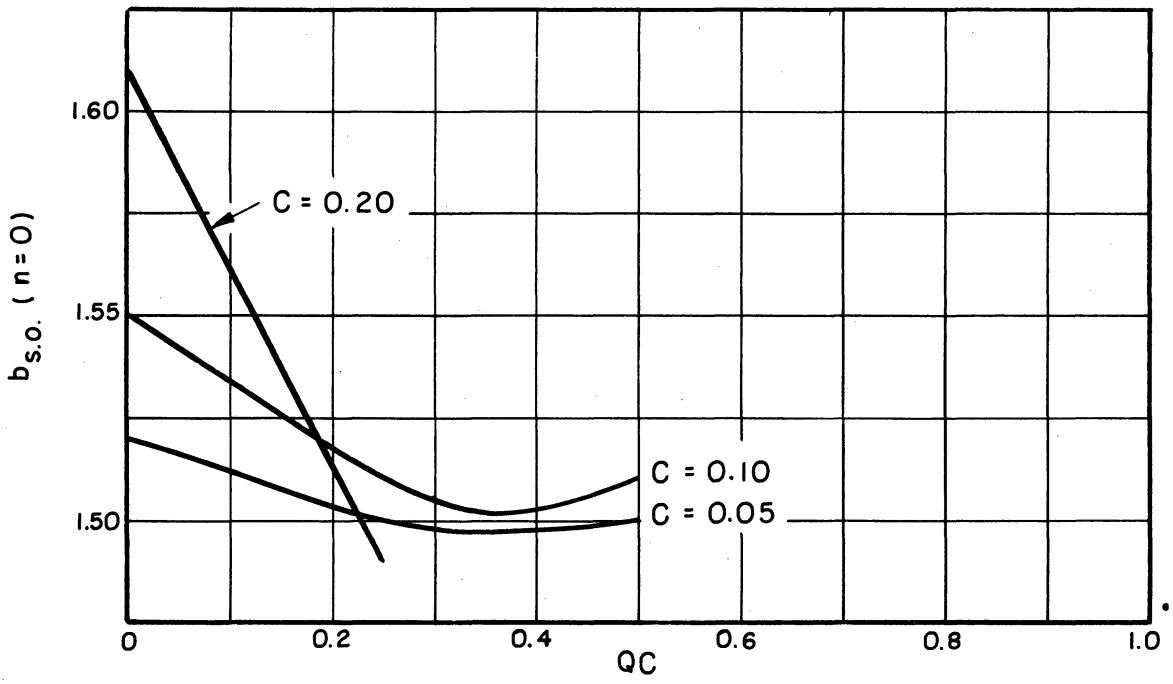

b. $b_{s.o.}$ VS. QC.

FIG. 10 LENGTH AND INJECTION VELOCITY AT LEAST START-OSCILLATION CURRENT IN A NONLINEAR BWO. (B = 1.0, d = 0)

minimum starting current can be expressed as

$$\frac{I_o}{I_s} = \left(\frac{CN}{(CN)_{I_s}}\right)^3 , \tag{23}$$

where I_o = stream current and

I_s = minimum start-oscillation current.

The efficiency is calculated using the following well-known relation:

$$\eta = 2CA_o^2 , \tag{24}$$

where A_o is the normalized value of the r-f voltage at the gun end of the device.

A composite plot of efficiency vs. I_o/I_s is shown in Fig. 11 for representative values of C and QC where circuit loss is neglected. The efficiency is seen to increase with increasing stream current up to a value of I_o/I_s of 1.8 and then levels off for all values of C and QC investigated. Increasing C produces an increased efficiency but increasing the space-charge parameter results in a decreasing efficiency. An increase of C from 0.05 to 0.10 results in an approximate doubling of the efficiency. For the case of C = 0.05 and QC = 0.25 a start-oscillation condition was found at $I_o/I_s = 4.3$.

The values of CN_s and b as functions of I_o/I_s corresponding to the data shown in Fig. 11 are shown in Fig. 12. It is seen that as the value of I_o/I_s is increased the value of b approaches a limiting value. These higher-current oscillation conditions indicate increasing output and are extremely difficult to locate since for large values of b the tube is relatively long

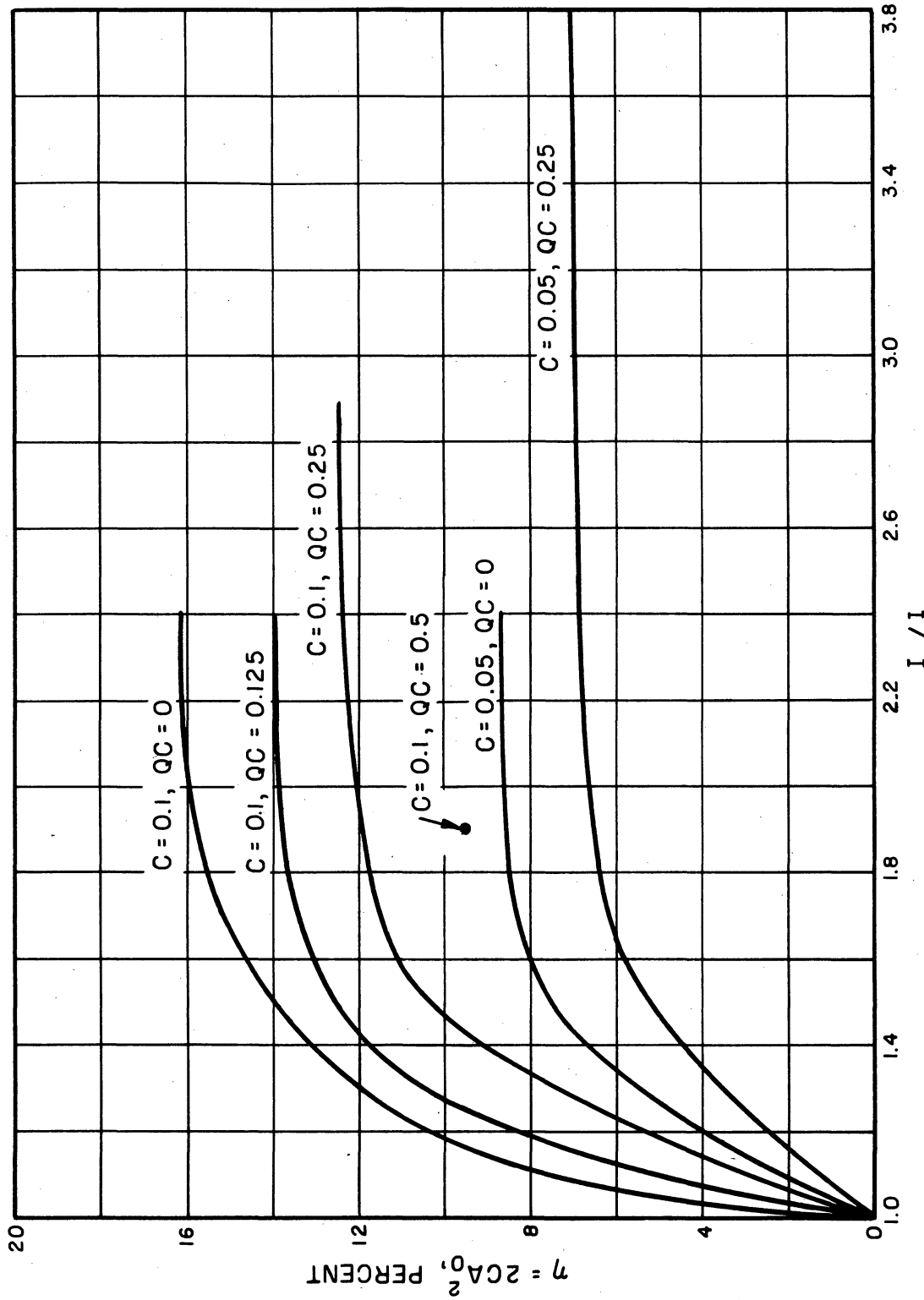

FIG. 11 EFFICIENCY VS. I_0/I_s WITH b ADJUSTED FOR OSCILLATION.
(B = 1.0, d = 0)

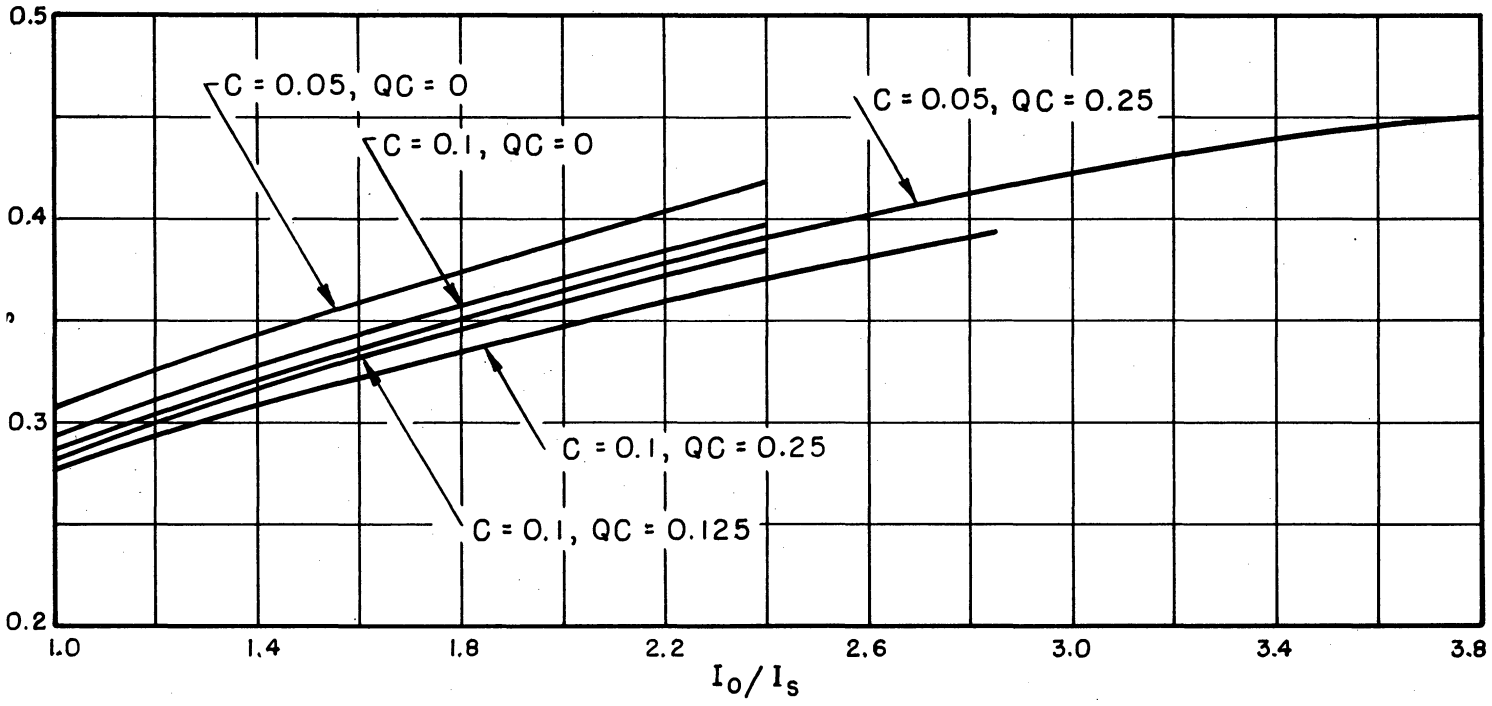

a. CN_s VS. I_o/I_s

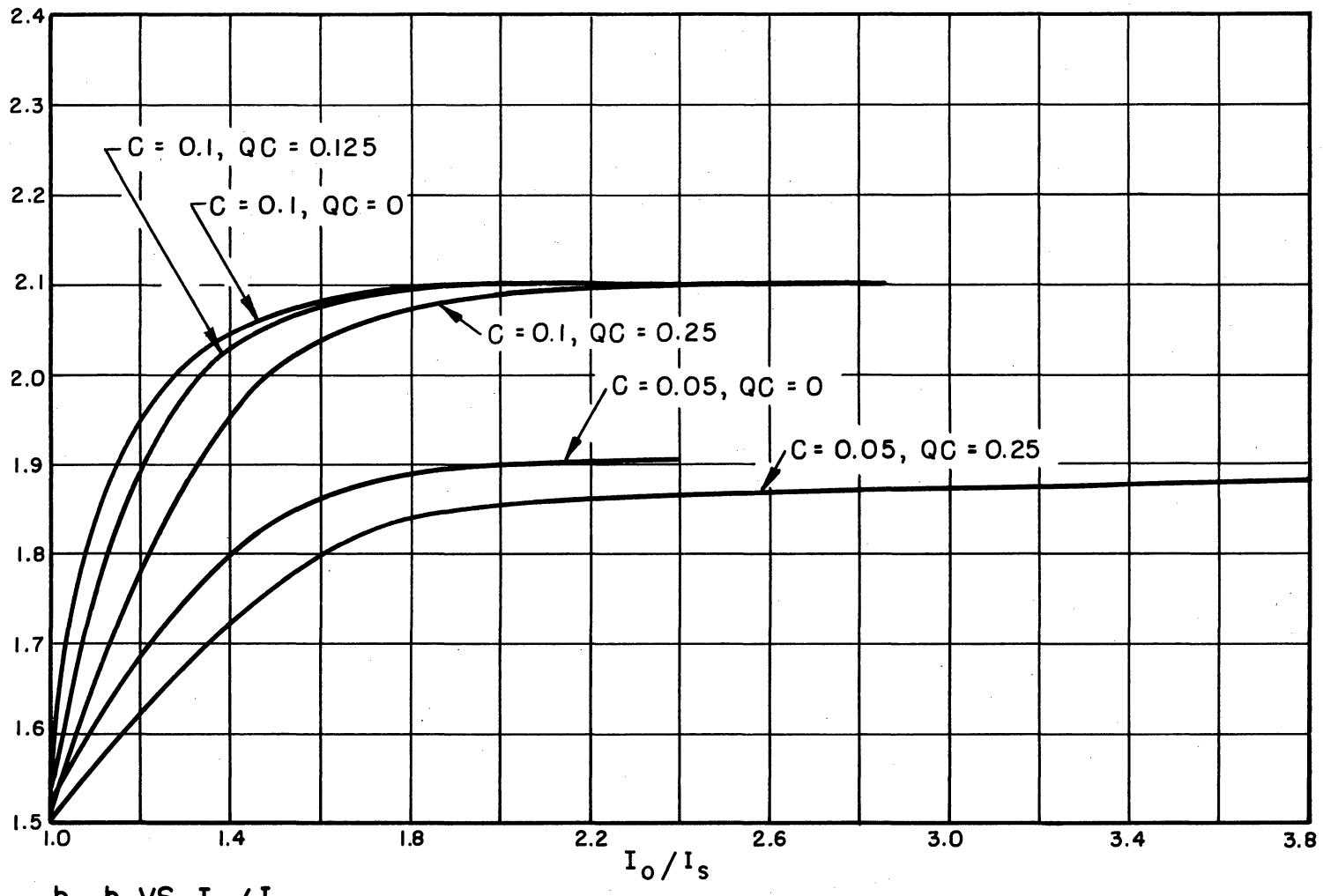

b. b VS. I_o/I_s

FIG. 12 CN_s AND b VS. I_o/I_s WITH b ADJUSTED FOR OSCILLATION.
(B = 1.0, d = 0)

and behaves much like a long line in the sense that the oscillation condition is very sensitive to the value of A_o. The value of CN at start oscillation is seen to increase smoothly as I_o/I_s is increased and probably becomes asymptotic to some limiting value at high stream currents.

Very high-order oscillation conditions have been observed in the calculations when the circuit voltage goes through zero to negative values and then increases to cross the zero axis again. This occurs at very large values of CN and these oscillation conditions would correspond to 80 to 100 times the minimum start-oscillation current.

Solutions were also found that decreased to a nonzero minimum and then increased and went through subsequent maxima and minima, one of which was zero. When C = 0.2 and QC = 0 it was found that the CN_s length decreased as b was increased (up to b = 2.3), indicating that for this large a value of C the length is not independent of the value of current and hence the cube relationship cannot be used. These results are shown in Fig. 13.

When C is small, say up to 0.1, it can be determined from a Fourier analysis of the electron velocity variation with distance that the average stream velocity changes slowly with distance and is not significantly reduced at the collector end compared to its initial value. Thus it is seen that the number of stream or circuit wavelengths in a given length is independent of I_o, u_o being relatively constant. The efficiency for C = 0.2 is not appreciably increased over the values obtained when C = 0.1. Values of C = 0.2 are very difficult to achieve practically and for this reason extensive calculations were not carried out for this high value of the gain parameter.

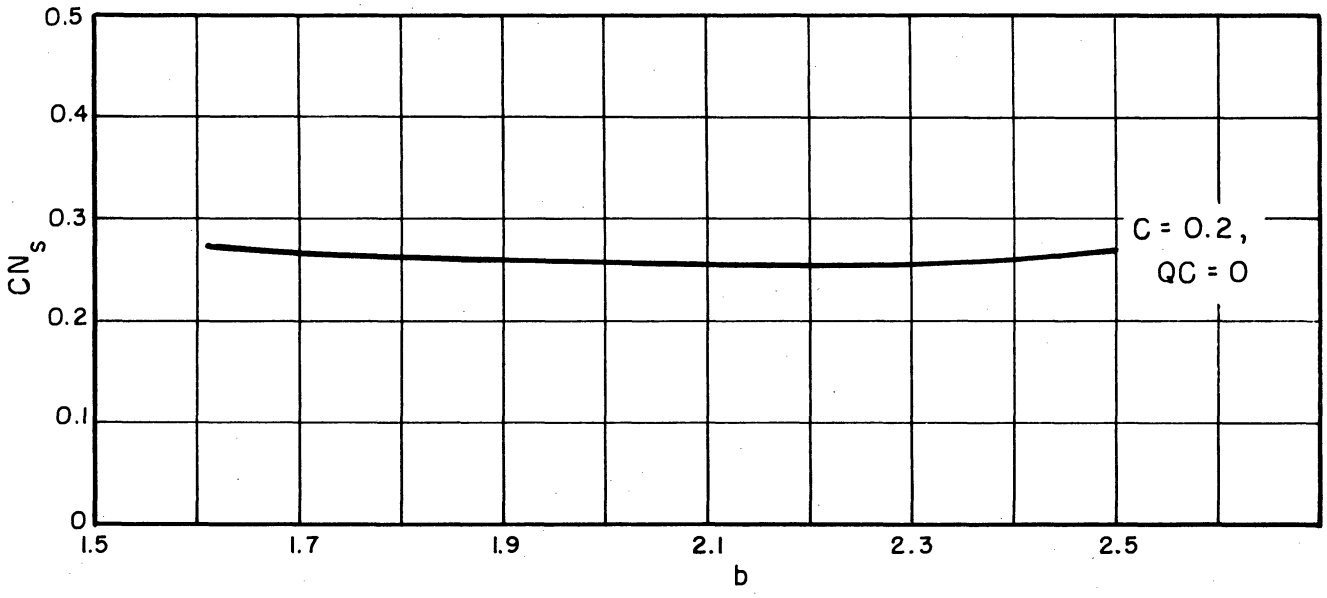

a. CN_s VS. b.

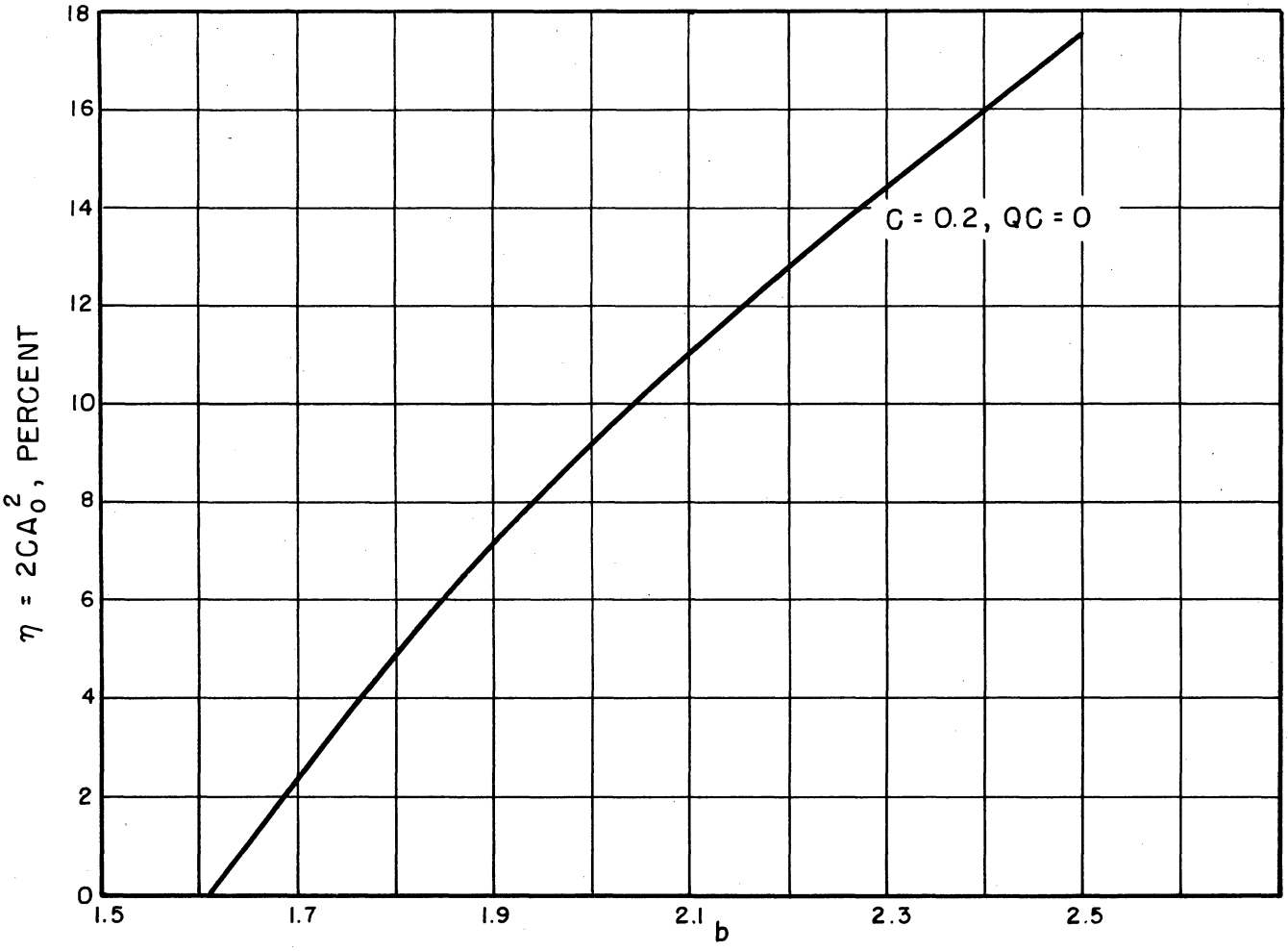

b. EFFICIENCY VS. b

FIG. 13 CN_s AND EFFICIENCY AT START OSCILLATION VS. b.

(C = 0.2, QC = 0, d = 0, B = 1.0)

The value of the ratio of fundamental current to d-c current in the stream depends on the level of oscillation generally increasing as the value of b and hence I_o/I_s is increased. For oscillation levels above the lowest oscillation condition it varies from 1.2 to 1.4, depending upon the values of C and QC. This is approximately midway between the values of 1 and 2 respectively used by Grow and Watkins[8] in computing efficiency from a linear theory. A value of the stream diameter B = 1 was used in the calculations, which corresponds to a fairly large beam; hence the efficiency results should probably be modified to account for variation of the circuit field across the stream.

The problem of solving the backward-wave device equations including the effects of radial electric field variation of the circuit field and the space-charge field is a formidable one. The results of Grow and Watkins[9] in estimating the decrease in efficiency due to radial field variations can probably be applied here and indicate that the efficiency is reduced by a factor of 0.8 when B = 1. Other effects such as circuit loss and velocity spread in the stream will also reduce the efficiency from that calculated here. The efficiency results calculated here are in good agreement with the efficiency data of Putz and Luebke[10] as reported by Grow and Watkins. Their experimental values of efficiency indicate a spread of data for η/C vs. $\omega_q/\omega C$ between 1.0 and 2.0 with a clustering around 1.5. These experimental data correspond to operating efficiencies around 8-10 percent and values of QC between 0.2 and 0.6.

---

8. See reference 3.

9. Op cit.

10. See reference 11.

CONCLUSIONS

The large-C linear O-type backward-wave oscillator equations have been derived and some interesting facets of their solution have been presented and discussed. Graphs of constant-gain contours and gain vs. length plots for various values of the circuit and stream parameters are given.

The nonlinear backward-wave oscillator equations were presented as modifications of the nonlinear forward-wave device equations and their method of solution was discussed. The start-oscillation values of CN and b were calculated for small values of output and found to check the small-signal calculations quite well. Efficiency and CN for values of I_o/I_s greater than one were calculated for a wide range of C and QC and the results were found to agree well with published experimental results on backward-wave oscillator efficiency.

ACKNOWLEDGMENTS

The author acknowledges the benefit of discussions, during the course of this work, with his associates in the Electron Tube Laboratory and in particular the assistance of Messrs. L. E. Stafford and Y. C. Lim in solving the equations on the computer. The General Motors Corporation also contributed computation time on their computer to the project.

Note:

At the time of writing of this report it was pointed out to the author by Dr. W. Veith of the Siemens and Halske Company of Munich, Germany, that he had obtained experimental data on efficiency vs. stream current that

verified the nature of the efficiency curves shown in Fig. 11. The efficiency values were lower due to a much lower circuit impedance and hence very small value of C. These results may be seen in "Das Carcinotron, ein Elektrisch Durchstimmbarer Generator für Mikrowellen", Fernmeldetechnische Zeitschrift, Bd. 7 (1954); pp. 23-27.

LIST OF SYMBOLS

A_o	normalized amplitude of the r-f voltage at the input
$A(y)$	normalized amplitude of r-f voltage along the structure
$B = \gamma b'$	stream-diameter parameter
b	injection velocity parameter
C	gain parameter
d	loss parameter
$F(\phi-\phi')$	space-charge field weighting function
I_o	stream current
I_s	minimum start-oscillation current
$\tilde{i}$	r-f convection current in the beam
QC	space-charge parameter
R	plasma frequency reduction factor
$u_t(y,\phi_o)$	total electron velocity
V	input r-f voltage amplitude
V_{ci}	circuit component of wave amplitude
V_i	total wave voltage amplitude
$V(z,t)$	amplitude of r-f voltage on the circuit
$\tilde{v}$	r-f velocity in the beam
v_g	wave group velocity
v_o	characteristic phase velocity of the circuit
v_p	wave phase velocity
$y = 2\pi CN_s = \theta$	normalized distance
Z_o	characteristic impedance of the circuit

LIST OF SYMBOLS
(Continued)

$\beta = \frac{\omega}{v}$	wave phase constant
$\beta_e = \frac{\omega}{u_o}$	stream phase constant
Γ	wave propagation constant in the presence of the beam
Γ_1	wave propagation constant in the absence of the beam
$\delta_i = x_i + jy_i$	wave incremental propagation constant
$\eta = 2CA_o^2$	efficiency
$\theta = 2\pi CN$	radian length of the tube
$\theta(y)$	phase shift of the r-f wave relative to a wave whose phase velocity is u_o
$\rho(z,t)$	space-charge density
$\phi(y,\phi_o)$	phase of the r-f wave on the circuit relative to the wave at the input
$\phi_o = \omega t_o$	entrance phase of the electrons relative to the r-f wave
ω	angular frequency
ω_p	radian electron-plasma frequency
$\omega_q = R\omega_p$	effective electron-plasma frequency

REFERENCES

1. Bernier, J., "Essai de Theorie du Tube Electronique a Propagation D'Onde", Ann. Radioelect., Vol. 2, pp. 87-101; January, 1947.

2. Goldberger, A.K., Palluel, P., "The O-Type Carcinotron", Proc. IRE, Vol. 44, pp. 333-345; March, 1956.

3. Grow, R., Watkins, D.A., "Backward-Wave Oscillator Efficiency", Proc. IRE, Vol. 43, pp. 848-856; July, 1955.

4. Harman, W.A., "Backward-Wave Interaction in Helix Type Tubes", Tech. Rpt. No. 13, Stanford University Electronics Laboratory; April, 1954.

5. Heffner, H., "Analysis of the Backward-Wave Traveling-Wave Tube", Proc. IRE, Vol. 42, pp. 930-937; June, 1954.

6. Johnson, H.R., "Backward-Wave Oscillators", Proc. IRE, Vol. 43, pp. 684-697; June, 1955.

7. Kompfner, R., Williams, N.T., "Backward-Wave Tubes", Proc. IRE, Vol. 41, pp. 1602-1611; November, 1953.

8. Muller, M., "Traveling-Wave Amplifiers and Backward-Wave Oscillators", Proc. IRE, Vol. 42, pp. 1651-1658; November, 1954.

9. Nordsieck, A., "Theory of the Large-Signal Behavior of Traveling-Wave Amplifiers", Proc. IRE, Vol. 41, pp. 630-637; May, 1953.

10. Pierce, J.R., Traveling-Wave Tubes, D. Van Nostrand Company, Inc., New York, New York; 1950.

11. Putz, J.L., Luebke, W.R., "High-Power S-Band Backward-Wave Oscillator", Tech. Rpt. No. 182-1, Stanford University Electronics Laboratory; February, 1956.

12. Rowe, J.E., "A Large-Signal Analysis of the Traveling-Wave Amplifier: Theory and General Results", Trans. PGED-IRE, Vol. ED-3, pp. 39-57; January, 1956.

13. Sedin, J., I.R.E. Conference on Electron Devices, Denver, Colorado; June, 1956.

14. Tien, P.K., "Bifilar Helix for Backward-Wave Oscillators", Proc. IRE, Vol. 42, pp. 1137-1143; July, 1954.

15. Walker, L.R., "Starting Currents in the Backward-Wave Oscillator", Jour. Appl. Phys., Vol. 24, pp. 854-860; July, 1953.

REFERENCES
(Continued)

16. Warnecke, R., Guenard, P., and Doehler, O., "Phenomenes Fondamentaux dans les Tubes a Onde Progressive", L'Onde Electrique, Vol. 34, pp. 323-338; April, 1954.

17. Watkins, D.A., Ash, E.A., "The Helix as a Backward-Wave Circuit Structure", Jour. Appl. Phys., Vol. 25, pp. 782-790; June, 1954.

18. Watkins, D.A., Rynn, N., "Effect of Velocity Distribution on Traveling-Wave Tube Gain", Jour. Appl. Phys., Vol. 25, pp. 1375-1379; November, 1954.

19. Weglein, R.D., "Backward-Wave Oscillator Starting Conditions", Trans. PGED-IRE, Vol. ED-4, No. 2, pp. 177-180; April, 1957.

DISTRIBUTION LIST

No. Copies	Agency
3	Commander, Rome Air Development Center, ATTN: RCERRT, Griffiss Air Force Base, New York
1	Commander, Rome Air Development Center, ATTN: RCSSTW, Griffiss Air Force Base, New York
1	Commander, Rome Air Development Center, ATTN: RCSSLD, Griffiss Air Force Base, New York
12	Armed Services Technical Information Agency, Documents Service Center, Arlington Hall Station, Arlington 12, Virginia
1	Commander, Air Force Cambridge Research Center, ATTN: CRQSL-1, Laurence G. Hanscom Field, Bedford, Massachusetts
1	Director, Air University Library, ATTN: AUL-7736, Maxwell Air Force Base, Alabama
2	Commander, Wright Air Development Center, ATTN: WCOSI-3, Wright-Patterson Air Force Base, Ohio
2	Commander, Wright Air Development Center, ATTN: WCOSR, Wright-Patterson Air Force Base, Ohio
1	Air Force Field Representative, Naval Research Laboratory, ATTN: Code 1010, Washington 25, D. C.
1	Chief, Naval Research Laboratory, ATTN: Code 2021, Washington 25, D. C.
1	Chief, Bureau of Ships, ATTN: Code 312, Washington 25, D. C.
1	Commanding Officer, Signal Corps Engineering Laboratories, ATTN: Technical Reports Library, Fort Monmouth, New Jersey
1	Chief, Research and Development Office of the Chief Signal Officer, Washington 25, D. C.
1	Commander, Air Research and Development Command, ATTN: RDTDF, Andrews Air Force Base, Washington 25, D. C.
1	Commander, Air Research and Development Command, ATTN: RDTC, Andrews Air Force Base, Washington 25, D. C.
1	Director, Evans Signal Laboratory, Belmar, New Jersey, ATTN: Mrs. Betty Kennett, Report Distribution Unit, Electron Devices Division
1	Chief, European Office, Air Research and Development, Shell Building, 60 Rut Cantersteen, Brussels, Belgium

DISTRIBUTION LIST
(Continued)

No. Copies	Agency
1	Secretariat, Advisory Group on Electron Tubes, 346 Broadway, New York 13, New York
1	California Institute of Technology, Department of Electrical Engineering, Pasadena, California, ATTN: Prof. L. M. Field
1	University of California, Electrical Engineering Department, Berkeley 4, California, ATTN: Prof. J. R. Whinnery
1	University of Colorado, Department of Electrical Engineering, Boulder, Colorado, ATTN: Prof. W. G. Worcester
1	Cornell University, Department of Electrical Engineering, Ithaca, New York, ATTN: C. Dalman
1	General Electric Company, Electron Tube Division of Research Laboratory, The Knolls, Schenectady, New York, ATTN: Dr. E. D. McArthur
1	General Electric Microwave Laboratory, 601 California Avenue, Palo Alto, California, ATTN: Technical Library
1	Huggins Laboratories, 711 Hamilton Avenue, Menlo Park, California, ATTN: L. A. Roberts
1	Hughes Aircraft Company, Electron Tube Laboratory, Culver City, California, ATTN: J. T. Milek
1	Varian Associates, 611 Hansen Way, Palo Alto, California, ATTN: Technical Library
1	Philips Research Laboratories, Irvington on the Hudson, New York, ATTN: Dr. Bernard Arfin
1	Columbia University Radiation Laboratory, 538 West 120th Street, New York 27, New York, ATTN: Technical Library
1	University of Illinois, Department of Electrical Engineering, Electron Tube Section, Urbana, Illinois
1	University of Florida, Department of Electrical Engineering, Gainsville Florida
1	John Hopkins University, Radiation Laboratory, Baltimore 2, Maryland, ATTN: Dr. D. D. King
1	Sperry Rand Corporation, Sperry Electron Tube Division, Gainsville, Florida, ATTN: Technical Library

DISTRIBUTION LIST
(Continued)

No. Copies	Agency
1	Stanford University, Microwave Laboratory, Stanford, California, ATTN: Dr. M. Chodorow
1	Stanford University, Stanford Electronics Laboratories, Stanford, California, ATTN: Dr. D. A. Watkins
1	Raytheon Manufacturing Company, Microwave Power Tube Division, Waltham, Massachusetts, ATTN: Technical Library
1	Federal Telecommunications Laboratories, Inc., 500 Washington Avenue, Nutley, New Jersey, ATTN: Technical Library, Electron Tube Laboratory
1	RCA Laboratories, Electronics Research Laboratory, Princeton, New Jersey, ATTN: Dr. E. H. Herold
1	Eitel-McCullough, Inc., San Bruno, California, ATTN: Mr. Donald Priest
1	Litton Industries, 960 Industrial Road, San Carlos, California, ATTN: Dr. Norman Moore
1	Massachusetts Institute of Technology, Research Laboratory of Electronics, Cambridge 39, Massachusetts, ATTN: Documents Library
1	Sperry Gyroscope Company, Great Neck, New York, ATTN: Engineering Library
1	Polytechnic Institute of Brooklyn, Microwave Research Institute, Brooklyn, New York, ATTN: Technical Library
1	Harvard University, Cruft Laboratory, Cambridge, Massachusetts, ATTN: Technical Library
1	Sylvania Microwave Tube Laboratory, 500 Evelyn Avenue, Mountain View, California, ATTN: Dr. D. Goodman
1	Sylvania Electric Products, Inc., Physics Laboratory, Bayside, New York, ATTN: Dr. R. G. E. Hutter
1	Bell Telephone Laboratories, Inc., Murray Hill Laboratory, Murray Hill, New Jersey, ATTN: Dr. J. R. Pierce
1	University of Washington, Department of Electrical Engineering, Seattle 5, Washington, ATTN: A. E. Harrison
1	Massachusetts Institute of Technology, Lincoln Laboratory, Lexington 73, Massachusetts, ATTN: Mr. Robert Butman